

Deep Smart Contract Intent Detection

Youwei Huang^{1,2}, Tao Zhang^{1,*}, Sen Fang¹, Youshuai Tan¹ and Jiachun Tao²

¹Macau University of Science and Technology, Macao SAR

²Institute of Intelligent Computing Technology, Suzhou, CAS, China

huangyw@iict.ac.cn

*corresponding author

Abstract—Nowadays, security activities in smart contracts concentrate on vulnerability detection. Despite early success, we find that developers’ intent to write smart contracts is a more noteworthy security concern because smart contracts with malicious intent have caused significant financial loss. Unfortunately, current approaches to identify the aforementioned malicious smart contracts rely on smart contract security audits, which entail huge manpower consumption and financial expenditure. To resolve this issue, we propose a novel deep learning-based approach, SMARTINTENTNN (Smart Contract Intent Neural Network), to conduct automated smart contract intent detection.

SMARTINTENTNN consists of three primary parts: a pre-trained sentence encoder to generate the contextual representations of smart contracts, a K-means clustering method to highlight intent-related representations, and a bidirectional LSTM-based (long-short term memory) multi-label classification network to predict the intents in smart contracts. To evaluate the performance of SMARTINTENTNN, we collect more than 40,000 smart contracts and perform a series of comparison experiments with our selected baseline approaches. Our experimental results demonstrate that SMARTINTENTNN outperforms all baselines by up to 0.8212 in terms of the f1-score metric.

Index Terms—Smart Contract, Intent Detection, Automated Software Engineering, Deep Learning

I. INTRODUCTION

Web3 is a technical term [1]–[3] that Gavin Wood¹ firstly coined under the context of Ethereum [4]–[6], it refers to decentralized applications (DApps) that run on the blockchain [7]. As an infrastructure for DApp development, a smart contract is defined as a computer program and a transaction protocol to automatically execute, control, or document legally relevant events and actions according to the terms of a contract or an agreement [8]–[13]. Generally, users can interact with smart contracts by sending transactions to invoke functions. From the perspective of computer programs, current studies on the security of smart contracts mainly focus on the detection of vulnerability or defect. However, as transaction protocols, smart contracts can also contain malicious intentions. Based on the above two natures of smart contracts, we divide the risks of smart contracts into two categories: external risks and internal risks.

What are external risks? If we analyze smart contracts from the perspective of computer programs, their risks are mainly concentrated in vulnerability exploitation [14]. Several vulnerable smart contracts exploited by attackers have been extensively studied, such as the infamous DAO attack caused

by *reentrancy vulnerabilities* [15], inconsistencies bugs led by *unchecked exceptions* [16]–[18], and making an invalid account balance or creating an infinite loop by *integer overflow or underflow* of a variable [19]. More vulnerabilities in smart contracts are summarized by *He et al.*’s team [20]. In addition to vulnerability exploitation, DoERS (Denial of Ethereum RPC service) is another attack behavior against node services in a blockchain network, which can drop the remote procedure call (RPC) service [21]. We regard the above types of attacks from the external of DApps by exploiting the weaknesses of smart contract code or blockchain network service as external risks.

```
function changeTax(  
    uint8 buyTax,  
    uint8 sellTax  
) public onlyOwner {  
    _buyTax = buyTax;  
    _sellTax = sellTax;  
}  
  
function setupEnableTrading() public onlyOwner {  
    tradingEnabled = true;  
}  
  
function setupDisableTrading() public onlyOwner {  
    tradingEnabled = false;  
}  
  
function teamUpdateLimits(  
    uint256 newBalanceLimit,  
    uint256 newSellLimit,  
    uint256 newBuyLimit  
) public onlyOwner {  
    balanceLimit = newBalanceLimit;  
    sellLimit = newSellLimit;  
    buyLimit = newBuyLimit;  
}
```

Fig. 1. Some code snippets of a smart contract, where the developer embeds several functions with intentional risks. Binance smart chain address: 0xDDa7f9273a092655a1cF077FF0155d64000ccE2A.

What are internal risks? In a real-life scene, malicious terms generally exist in legal contracts which can cause the loss of users’ interests. Considering that the smart contract is a transaction protocol designed by human beings, we find that harmful terms also exist in smart contracts, in the form of computer code. According to our investigation, in recent years, more and more risks are intentionally designed by smart contract developers or DApp creators themselves [22], [23]. A scam DApp purposely injects malicious code, such as tricks and backdoors, into the smart contracts to misappropriate users’ funds [24]. As shown in Fig. 1, it gives

¹<https://gavwood.com>

several intentional risk samples in a real-world smart contract. From the figure, we can observe that all functions contain the same modifier: *onlyOwner*, which means that they are ownership centralized. For instance, if adding the modifier *onlyOwner* to the function *changeTax*, a development team can, and only they can, arbitrarily change the tax fee for swapping the assets in a smart contract. Similar to *changeTax*, *teamUpdateLimits* added *onlyOwner* can give the developer the right to modify various limits for transactions. As for the remaining two functions, they express an even more dangerous development intent that allows the owner directly turn on or off the trading function in the smart contract. We define these risks owing to developers' malicious intents as internal or intentional risks.

What is our research? Internal risks of smart contracts have caused more and more economic losses, but the current detection of malicious smart contracts relies on smart contract security audits, which entail huge manpower consumption and financial expenditure [25]. Unfortunately, all existing work focuses on the research of external risks of smart contracts by detecting and exploiting the smart contract vulnerabilities or blockchain network defects. It motivates us to propose a new approach to implement automated smart contract intent detection, to detect whether a smart contract is injected with malicious intents by developers as well as distinguish these intents. Specifically, we present SMARTINTENTNN, a deep learning model that combines sentence embedding, intent highlight, and bidirectional long-short term memory (BiLSTM) [26], [27]. SMARTINTENTNN is a multi-label classification model implemented with Tensorflow.js [28], [29] that can detect ten categories of malicious intents (see details in Table I) in smart contracts, by retrieving their contextual information.

To evaluate the performance of SMARTINTENTNN, we collect a dataset with more than 40,000 smart contracts developed in Solidity [30], each of which is labeled with none or multiple malicious intents. Before passing smart contracts into our model, we perform pre-processing on it, including removing non-logic code, removing comments, and generating the code tree for each smart contract. Then, we utilize a pre-trained sentence encoder [31] to transfer each *function* in smart contracts into a context vector that can be further learned by neural networks. To help the neural network learn the representations better, we pre-train an intent highlight model based on K-means to predict the strength of the intent in smart contracts. Finally, we perform the multi-label classification for smart contracts through a deep neural network (DNN). We compare SMARTINTENTNN with other baseline models, *e.g.*, LSTM, and the experimental results demonstrate that SMARTINTENTNN outperforms all compared approaches with the highest f1-score metric of **0.8212** and can effectively identify smart contracts with malicious intents as well as point out their types.

Our contributions can be listed as the following points:

- To the best of our knowledge, this is the first work to propose an approach to implement automated smart

contract intent detection, which can detect developers' risky intents injected in a smart contract;

- We utilize a universal sentence encoder, an intent highlight model based on K-means, and a BiLSTM-based DNN to implement the automated approach for smart contract intent detection, namely SMARTINTENTNN;
- We collect an extensible dataset of smart contracts with intent labels for smart contract intent learning;
- We publish our research source codes, datasets and documents².

II. MOTIVATION

Why is it essential to identify the developers' intent in smart contract development? – For the love of money is the root of all evil. In conventional web software development, developers' intent is a rarely mentioned concept since conventional applications are released by a trustable centralized party. They are responsible for processing the code logic and guaranteeing the software quality. Additionally, conventional applications make money by providing high-quality software services to users, and they do not build their cryptocurrency systems. By contrast, Web3 applications are decentralized and value-driven, which means that any developer can deploy a smart contract and promote it to users for financial purposes. More importantly, smart contracts contain their own economic systems, which are tied to real-value cryptocurrencies (*e.g.*, Bitcoin), which may have a potential risk: when a smart contract reaches a high value³, greedy developers can steal or dump users' crypto value by executing the preset malicious code. Therefore, in DApp development, the developers' intent is worth our attention.

Did the developer's malicious intent really cause financial damage? According to the statistics from 2022 crypto crime report from Chainalysis [32], cryptocurrency-oriented scammers have stolen around \$7.8 billion worth of cryptocurrency from victims, over \$2.8 billion of which is from rug pulls. A rug pull means that developers conduct unfair transactions by invoking the preset malicious functions injected in smart contracts, to illegally withdraw the funds from a smart contract address, or unpair the liquidity pool and appropriate the valuable part [33]. Compared to the statistics released in 2020, the losses in 2021 rise 82%. *Torres et al.*'s investigation has found that 690 smart contracts of honeypots bring an accumulated profit of more than \$90,000 for the creators. In the real world, most users are not experts, and they cannot understand any programming code. They just trust these DApps and invest in them, but eventually become the victims of these programs. Therefore, smart contracts with malicious intent can cause substantial economic losses to the users.

Why do we propose an automated intent detection tool for smart contracts? For a developer, reusing smart contract code, cloning code, and importing other contracts are common

²<https://gitlab.com/web3se/smartintent>

³A simple way to estimate the value of a smart contract is to calculate its TVL, referring to <https://learn.bybit.com/defi/total-value-locked-tvl>.

behaviors in Web3 development. To the development behavior with malicious intent, we think that it is necessary to develop an automated tool for supervising these developers, preventing such intents into real actions. Such an automated tool can also help developers to distinguish smart contracts from malicious intents when they reuse third-party smart contracts. Currently, the smart contract security audit is an effective way to identify malicious smart contracts. However, the audit service is incredibly expensive and time costly because it is manual work completed by experts. Thus an automated audit tool has the practical sense to reduce the development cost in terms of time, labor power, and money.

III. BACKGROUND

In this section, we introduce background knowledge, including smart contracts with malicious intents, sentence embedding, and bidirectional LSTM.

A. Malicious Smart Contract Intent

Smart contracts enable everyone to interact online via a blockchain network. Taking Ethereum blockchain, the most popular smart contract operation platform, as an example, we discuss how a developer grab benefits from the users by injecting malicious intents into a smart contract. Ethereum, or Ethereum-like blockchains are essentially transaction-based machines. Deploying smart contracts and invoking smart contracts are both transactions. Two types of addresses are stipulated on Ethereum: externally owned accounts (EOA) address and contract address. To complete a transaction, an EOA address pays a kind of native cryptocurrency, called ether (ETH) as the gas fee, which is the valuable crypto asset.

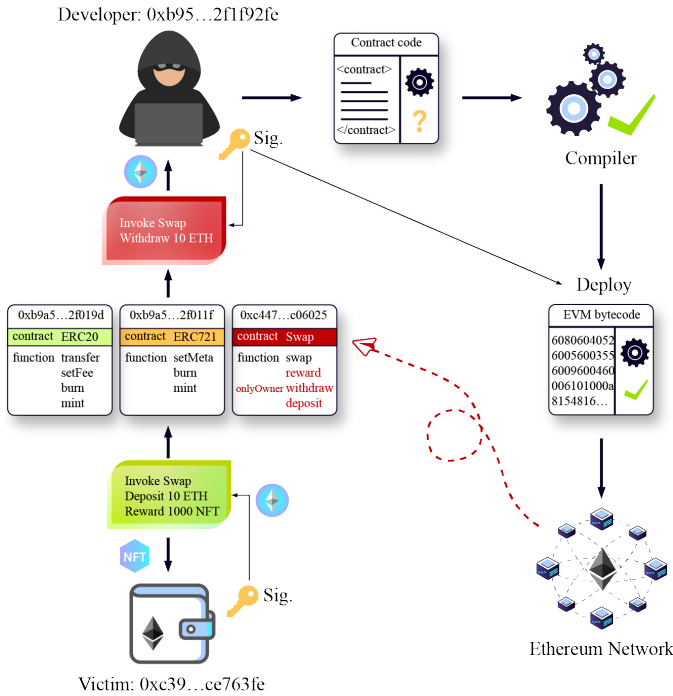


Fig. 2. A description of developers illegally grabbing benefits from users by developing and deploying smart contracts with malicious intents.

As indicated in Fig. 2, both a developer and a user own EOA addresses. The developer develops a smart contract and compiles it to the bytecode, a low-level computer language executable on Ethereum Virtual Machine (EVM) [34]. Then, the developer signs a transaction with a private key and sends it to deploy the bytecode to the Ethereum network. A smart contract address is generated after the transaction succeeds. There is a *reward* function implemented in this smart contract to attract users. This function allows users to stake ETH to harvest a certain amount of rewards, such as NFTs (non-fungible tokens) [35]. A user sends a transaction to invoke the *deposit* function and pays 10 ETH to the contract address. Then, the user invokes the *reward* function and receives the NFTs. However, the developer can easily steal the user's 10 ETH by invoking a *withdraw* function. All the above transactions are packaged into blocks and blocks are chained together through a cryptographic hash. As a result, the victim's money (ETH) can never be retrieved.

B. Sentence Embedding

Embedding (also known as distributed representation) [36] is a technique for learning dense representations of entities such as words, sentences, and images. Compared to word-level embeddings, such as word2vec [37] and GloVe [38], Universal Sentence Encoder (USE) is a sentence-level [39] encoder that generates sentence embeddings by aggregating the word representation in a sentence.

USE takes a sentence as the input and outputs a contextual representation of the sentence. It enables similar sentences to be close in its generated vector space [36], [40]. In this paper, we regard every *function* snippet in the smart contract as a sentence and pass it into USE to obtain the corresponding contextual representation.

There are two methods to design USE. One is designed on the transformer architecture [41] and targets high accuracy but has the greater cost of model complexity and resource consumption. Another one targets efficient inference with slightly reduced accuracy by making full use of a deep averaging network (DAN) [42].

C. Bidirectional LSTM

A common LSTM cell is composed of a memory cell, a forget gate [43], an input gate, and an output gate [44]. A cell remembers values over arbitrary time intervals and the three gates regulate the flow of information into and out of the cell. A bidirectional LSTM (BiLSTM) wraps two LSTM layers: one obtains the output in the forward order, and the other one obtains the output in the backward order. The output of a BiLSTM is the concatenation of outputs in the above two layers. Compared to LSTM which only learns the context dependency from the left of the input sequence, BiLSTM can learn the dependency from both sides of the input sequence. It makes BiLSTM significantly more effective in context semantic understanding than LSTM.

IV. DATASET

To train SMARTINTENTNN, we collect an unrepresented dataset of more than 40,000 smart contracts from the explorer of Binance Smart Chain (BSC)⁴ and label the intents for them. BSC is an Ethereum-like blockchain, smart contracts executing on BSC are compatible with Ethereum. Fig. 3 shows the process of data collection and preprocessing. We first download a large number of open-source smart contracts from the blockchain explorer. Then the smart contracts with multiple files are merged, and the redundant and noisy code snippets are dropped. Finally we apply the regular expression (Regex) to extract code snippets according to the Solidity keywords to generate a smart contract code tree.

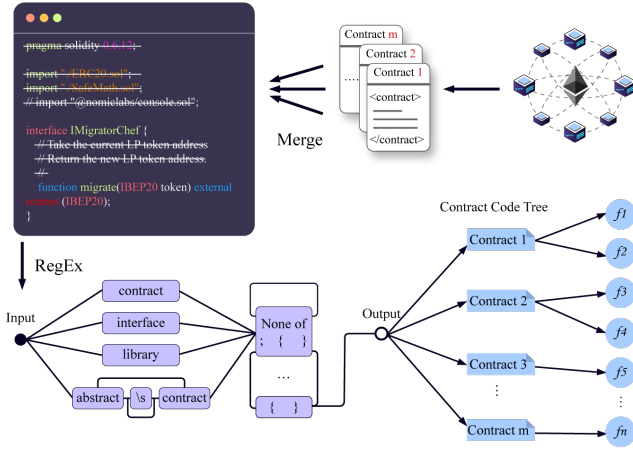


Fig. 3. Preprocess of dataset: (i) download the open-source smart contracts from the BSC blockchain and label them; (ii) clean the source code and generate the smart contract code tree.

A. Intent Labels

Ten categories of risky intents are labeled as shown in Table I. Our label resource comes from the StaySafu⁵ and the experience of DApp developers and auditors.

TABLE I
CATEGORIES OF RISKY INTENTS

Id	Intent	Percentage	Instance
1	fee	26.86%	<i>setFeeAddress(address)</i>
2	disableTrading	5.34%	<i>enableTrading(bool)</i>
3	blacklist	3.82%	<i>require(!isBlacklisted(sender))</i>
4	reflect	37.50%	<i>tokenFromReflection(uint256)</i>
5	maxTX	13.76%	<i>setMaxTxPercent(uint256)</i>
6	mint	8.53%	<i>mint(uint256)</i>
7	honeypot	0.23%	<i>require(allow[from])</i>
8	reward	3.37%	<i>updateDividendTracker(address)</i>
9	rebase	0.53%	<i>LogRebase(uint256, uint256)</i>
10	maxSell	0.05%	<i>setMaxSellToken(uint256)</i>

We explain the ten types of intents listed in Table I:

⁴<https://bscscan.com>

⁵<https://www.staysafu.org>

- 1 **Fee** aims to modify transaction fees. Fees paid by users for each transaction are transferred to a specified developer's wallet.
- 2 **DisableTrading** can directly turn on or off the trading action in a smart contract.
- 3 **Blacklist** restricts the behavior of its designated users on smart contracts. It undermines the interests of these users and prejudice their right to trade fairly and freely.
- 4 **Reflection** is usually financed by a percentage tax on any transaction. Taxes are redistributed to the holders according to the size of their holding tokens. It can be a gimmick to attract users to buy the native tokens which may not have any use case.
- 5 **MaxTX** can limit the maximum number or volume of transactions.
- 6 **Mint** allows issuing new tokens. This issue can be unlimited or artificially controlled.
- 7 **Honeypot** is a smart contract that pretends to leak its funds to a user, provided that the user sends additional funds to it. However, the funds provided by the user will be trapped and retrieved by the honeypot creator [22].
- 8 **Reward** is to reward users with specific crypto assets in the form of dividends to attract users to buy or use the native tokens. Similarly, these assets may not have value.
- 9 **Rebase**, or elastic, controls the token price by algorithmically adjusting the supply.
- 10 **MaxSell** limits the specified users' selling times or amounts, so that it can lock their liquidity.

Each of the above intents can appear more than once in a smart contract. From our statistical data, the most frequent intentional risk is **reflect**. In our dataset, **reflect** appears in 33,268 places over the 40,000 smart contracts, accounting for 37.5% of all the types of intents, followed by **fee** (26.86%) and **maxTX** (13.76%) respectively. The risk **maxSell** accounts for the least, only 0.05%, occurring in a total of 68 places in our dataset.

B. Code Mergence & Drop

The source code of the smart contract on BSC exists in two forms. One is a single-file smart contract, whose *import* contracts are merged by developers through a flattener tool before uploading. The other is a multi-file smart contract, whose code is separated into multiple files. For multi-file smart contracts, we merge multiple files into a single document.

The Solidity compiler version specification *pragma*, *import* statements, and *comments* in a smart contract are dropped out. The Solidity compiler version (*pragma*) does not express any developer's intent, and the *code comments* take no impact on the implementation of any intent. Since the external contracts in the *import* statements have been merged in the previous step (multi-file smart contracts), removing the *import* statements will not lose the intent information of a smart contract.

C. Smart Contract Code Tree

Since a smart contract is a document of computer code, we cannot directly feed it into a neural network. To extract the

model input data, we introduce the concept of a smart contract code tree (CCTree). A CCTree is a tree graph data structure generated by splitting and reorganizing a smart contract source code. As shown in Fig. 4, a CCTree is expanded into three layers: (i) the first layer is the root layer, representing the entire smart contract document; (ii) the second layer is the contract layer, representing the *contract* classes in a smart contract; (iii) the third layer is the function layer, representing the *function* context under a *contract* class. Only one node is placed in the root layer, denoted by \mathbf{T} . The second layer lists the *contract* classes in \mathbf{T} , including the class types of *contract*, *interface*, *library*, and *abstract contract*, denoted by \mathbf{C} . The third layer contains leaf nodes, which store the code snippets with the keywords of *function*, *event*, *modifier*, and *constructor* in the *contract* class, denoted by \mathcal{F} . Afterward, we can easily load any data, e.g., \mathbf{T} , \mathbf{C} and \mathcal{F} , from a CCTree on demand.

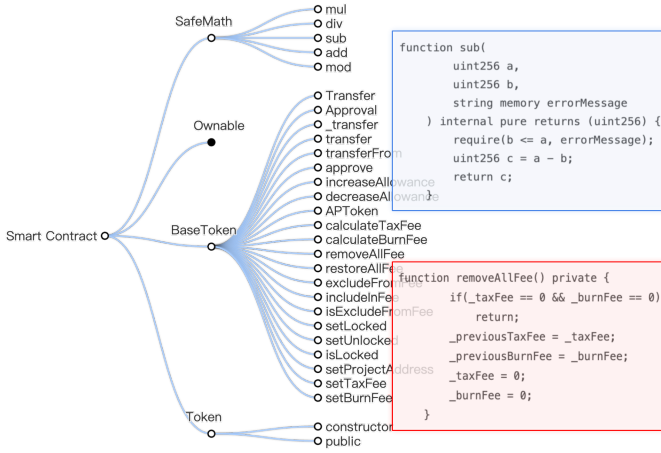


Fig. 4. The smart contract code tree generated from the BSC address: 0xe4d200e40c1fc483d2aedf0e97debd7ab5760351.

V. APPROACH

We introduce how we leverage the DNN-based approaches to detect the intents in smart contracts. Fig. 5 describes an overview of our approach, named SMARTINTENTNN, which could be divided into three primary parts: smart contract embedding, intent highlighting, and DNN learning. First, we encode smart contracts to embedding vectors through the universal sentence encoder. Then the intents of smart contracts are highlighted through a K-means model. Finally, we feed the highlighted data into the DNN to learn the representations of smart contracts and perform the multi-label classification on them. In this section, we explain our approach in details.

A. Smart Contract Embedding

To generate the embedding (contextual representation) of a smart contract, we first employ an encoder to generate the embeddings for each *function* in the smart contract. Then we combine all the *function* embeddings to represent the entire smart contract.

As we have introduced the CCTree in Section IV, we iterate all the leaf nodes in the CCTree. We use the pre-trained model USE based on the DAN architecture to encode each *function* \mathcal{F} (i.e., leaf node) in a smart contract into the sentence embedding. Formula 1 describes the embedding process, where Φ represents the contextual encoder and its input data \mathcal{F} can be any context of *function*. It outputs a vector \mathbf{f} which is the embedding of the *function* \mathcal{F} .

$$\Phi(\mathcal{F}) : \mathcal{F} \rightarrow \mathbf{f} \quad (1)$$

To generate a sentence embedding of \mathcal{F} , the following three steps are processed by DAN: (i) calculate the vector average of the word embeddings in a sentence; (2) pass the average vector through one or more feed-forward layers; (3) perform the classification in an activation layer to generate a universal sentence embedding.

$$\mathbf{T}(\mathcal{F}) : \mathcal{F} \rightarrow \mathbf{W}^{\mathcal{F}} = \{w_1, w_2, \dots, w_n\} \quad (2)$$

$$\phi(w_i) : w_i \in \mathbf{W}^{\mathcal{F}} \rightarrow \mathbf{w}_i \quad (3)$$

$$\mathbf{f}^0 = \frac{1}{n} \sum_{i=1}^n \mathbf{w}_i \quad (4)$$

Formula 2-4 describe the first step in DAN. \mathbf{T} in Formula 2 generates the word tokens from a sentence, which is usually named as “tokenizing”. The text of *function* \mathcal{F} is split into an ordered set $\mathbf{W}^{\mathcal{F}}$ of multiple word tokens $\{w_i\}_{i=1}^n$. In Formula 3, ϕ transfers tokens into word embeddings [36] $\{\mathbf{w}_1, \mathbf{w}_2, \dots, \mathbf{w}_n\}$. Eventually, Formula 4 averages all the word embedding vectors to \mathbf{f}^0 .

The intuition behind deep feed-forward neural networks means that each layer learns a more abstract representation of the input data than the previous one [45]. In the second step of DAN, the averaged output \mathbf{f}^0 is further transformed by multiple feed-forward layers. We assume taking n feed-forward layers, and each feed-forward layer can be illustrated by Formula 5. \mathbf{W}_i is a $k \times k$ weight matrix where k is the size (dimension) of vector \mathbf{f}^i . The activation function σ is usually sigmoid or tanh, and \mathbf{b}_i is a bias term.

$$\mathbf{f}^i = \sigma(\mathbf{W}_i \cdot \mathbf{f}^{i-1} + \mathbf{b}_i), i \in \{1, 2, \dots, n\} \quad (5)$$

In the third step, feeding \mathbf{f}^n to a softmax layer can generate the universal representation of the *function* \mathcal{F} . \mathbf{W}_s is an $m \times k$ weight matrix for the input of a k size vector and the output of a *function* embedding with m features. Formula 6 outputs \mathbf{f} , which is the embedding of the *function* context.

$$\mathbf{f} = \text{softmax}(\mathbf{W}_s \cdot \mathbf{f}^n + \mathbf{b}_s) \quad (6)$$

The above operations are performed on each *function* in a smart contract and we finally push their embedding vectors \mathbf{f} into \mathbf{X} to represent the entire smart contract. \mathbf{X} is an $n \times m$ matrix where n equals to the number of *functions* in a smart contract and m is the number of features in \mathbf{f} .

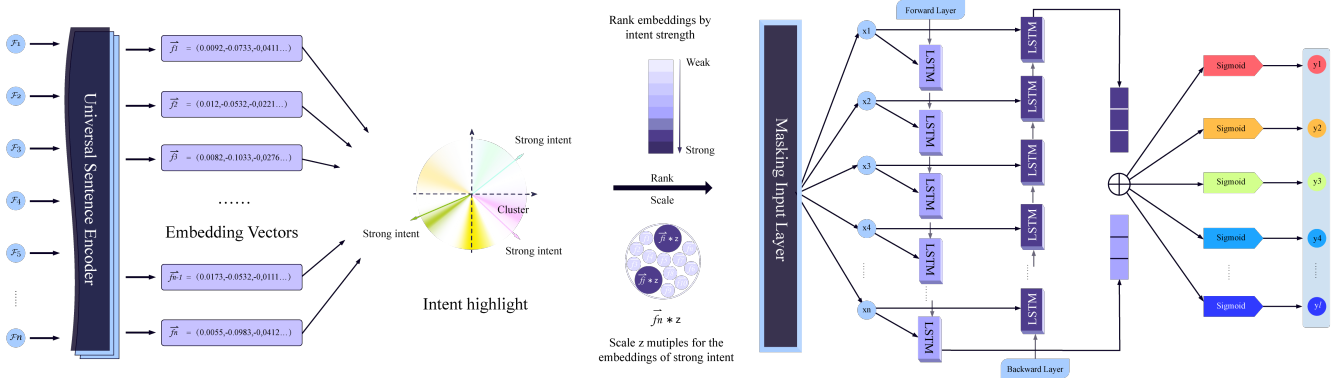


Fig. 5. The overview workflow of SMARTINTENTNN: (i) encode smart contracts through the universal sentence encoder; (ii) highlight the developers' intents in smart contracts through a K-means model; (iii) feed the intent highlighted data into a DNN to learn the representations of smart contracts. The architecture of our DNN: an input layer, a BiLSTM layer, and a dense layer for outputting the multi-label binary classification results.

B. Intent Highlight

Although we can directly feed X into a DNN, not all *functions* in a smart contract express the developer's intent. Thus, we present intent highlight to stress the intent-related *functions* in a smart contract. Intent highlight is a pre-trained model based on K-means machine learning [46], [47], aiming to predict the intent strength of each vector f in X . Formula 7 describes the intent highlight method, where H is an unsupervised model and its output is the intent-highlighted data X' .

$$H(X) : X \rightarrow X' \quad (7)$$

To get the k value of K-means, we compute the occurrence rate of each *function* \mathcal{F} . A *function* occurrence rate can be defined as the frequency of a *function* occurring in a smart contract dataset, described as $R(\mathcal{F})$ in Formula 8. We assume there is a sample of dataset S and there are m smart contracts in S , $S = \{T_i\}_{i=1}^m$. If the *function* \mathcal{F} exists in the tree T_i , it is denoted by $E(T_i, \mathcal{F}) = 1$ in Formula 9, and we count once for R . Eventually, we count the number of \mathcal{F} whose $R(\mathcal{F}) > \rho$ as the value of k . The threshold of the occurrence rate ρ will be fit in the experiment.

$$R(\mathcal{F}) = \frac{1}{m} \sum_{i=1}^m E(T_i, \mathcal{F}) \quad (8)$$

$$E(T, \mathcal{F}) = \begin{cases} 1 & \mathcal{F} \in T \\ 0 & \mathcal{F} \notin T \end{cases} \quad (9)$$

When comparing the similarity of two documents, we prefer to compute the cosine distance between their embedding vectors [48]. For example, there are two *functions* (\mathcal{F}_A and \mathcal{F}_B) whose embedding vectors are $f^A = [f_1^A, f_2^A, \dots, f_n^A]$ and $f^B = [f_1^B, f_2^B, \dots, f_n^B]$. Formula 10 provides a method for calculating the text similarity between \mathcal{F}_A and \mathcal{F}_B , that is, the cosine value of f^A and f^B . Therefore, we transform cosine similarity to cosine distance by Formula 11.

$$\begin{aligned} \cos \langle f^A, f^B \rangle &= \frac{f^A \cdot f^B}{\|f^A\| \|f^B\|} \\ &= \frac{\sum_{i=1}^n f_i^A \times f_i^B}{\sqrt{\sum_{i=1}^n (f_i^A)^2} \times \sqrt{\sum_{i=1}^n (f_i^B)^2}} \end{aligned} \quad (10)$$

$$D(f^A, f^B) = 1 - \cos \langle f^A, f^B \rangle \quad (11)$$

To find the centroid of each cluster for K-means, we assume a training dataset $\{f'_i\}_{i=1}^n$ with n samples of *contract functions* and k random means (centroids) $\{c_j^t\}_{j=1}^k$, $t = 0, 1, \dots, z$, where z represents the maximum number of iterations in K-means. K-means repeatedly performs the calculation of the minimum square Euclidean distance between the current centroids and each within-cluster observation value from the initial centroids $\{c_j^0\}_{j=1}^k$. We replace the squared Euclidean distance with the cosine distance mentioned above. Let us assign f'_i to its closest mean c_j^t and denote as a set M_j^t , where f'_i is a within-cluster observation value to c_j^t . In Formula 12, if f'_i is the within-cluster observation to c_j^t , the cosine distance between them is calculated, otherwise the distance is 0.

$$M(f'_i, c_j^t) = \begin{cases} D(f'_i, c_j^t) & f_j \in M_j^t \\ 0 & f'_i \notin M_j^t \end{cases} \quad (12)$$

$$c_j^{t+1} = \frac{\sum_{i=1}^n \frac{M(f'_i, c_j^t) f'_i}{D(f'_i, c_j^t)}}{\sum_{i=1}^n \frac{M(f'_i, c_j^t)}{D(f'_i, c_j^t)}} \quad (13)$$

$$\min \left\{ \sum_{j=1}^k \sum_{i=1}^n M(f'_i, c_j^t) \right\}_{t=0}^z \quad (14)$$

According to Formula 13, after each round, the centroid c_j^t is updated to c_j^{t+1} where $0 \leq t \leq z$. The training target is to minimize the total within-cluster variation (TWCV) as Formula 14. The training is terminated when t reaches the maximum iteration limit, z rounds, or the minimum TWCV is no longer significantly reduced. Eventually, we find the most appropriate centroids $\{c_j\}_{j=1}^k$ for K-means.

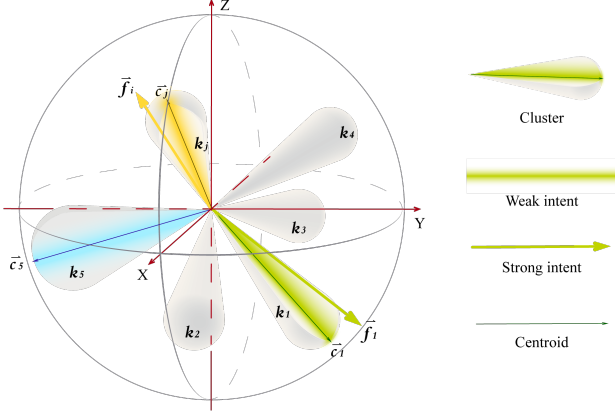


Fig. 6. Use a 3D coordinate system to describe the principle of intent highlight. The larger the vector angle deviates from the centroid in space, the stronger its intent is.

As the K-means model is ready, we can pass any vector f_i to predict its within-cluster distance. Around the centroids c_j in Fig. 6, we find some frequently occurring and similar *function* code snippets. Their vectors densely keep a short distance from the centroids. These code snippets are usually from public libraries, written with mainstream algorithms, or the codes in high-frequency reuse. We consider that these *functions* are as weak as to offer the developer’s intent while the centroid-outlying *functions* are distinctive, expressing the strong intent. Therefore, we regard a within-cluster distance as the strength of intent.

$$\mathbf{X}' = \text{rank}(\mathbf{X}) \text{ by } D(\mathbf{f}_i, \mathbf{c}_j) \quad (15)$$

$$\mathbf{X}' = \text{scale}(\mathbf{X}) \text{ by } \mu \mathbf{f}_i \text{ if } D(\mathbf{f}_i, \mathbf{c}_j) \geq \lambda \quad (16)$$

We rank or scale f_i in \mathbf{X} by the predicted within-cluster distance and generate a new matrix \mathbf{X}' . In Formula 15 and 16, $i \in \{1, 2, \dots, n\}$, $j \in \{1, 2, \dots, k\}$, λ is a threshold of the distance, beyond which, f_i can be scaled by μ times. The above steps can be found in the middle part of Fig. 5, nearby intent highlight.

C. Multi-label Classification

In this section, we introduce the last part of Fig. 5, using a DNN for multi-label classification. The architecture of the DNN can be divided into three layers: an input layer (masking layer), a bidirectional LSTM layer, and an output layer. To learn the classification, we feed the intent highlighted data, that is, the matrix (sequence) \mathbf{X}' output from the previous intent highlight model, to DNN.

The data first flows into the input layer, and we assume that the input layer accepts a sequence of $a \times b$ size. The number of *functions* \mathcal{F} input for each time should be equal to a . The vector size of each *function* embedding f_i is required to be equal to b . The size of the *function* embedding vector is fixed, for instance, USE outputs a vector of 512 units. Therefore, we do not need to make any change to the columns of \mathbf{X}' . We just need to ensure that b of the input layer is the same as the vector size of f_i . However, the row size of \mathbf{X}' is determined by the number of *functions* in each smart contract. There is a situation for \mathbf{X}' , where the number of its rows may be less than a . Such smart contracts are very simple as they usually contain very few *functions*. We pad the absent rows of \mathbf{X}' with zero vectors. Our input layer is also a masking layer. Tensorflow’s official explanation of the masking layer⁶ is that it can skip timesteps by giving a masking (skipping) value. Therefore, we set the masking value equal to the above padded value, which is 0.

The data flows into the second layer, a bidirectional LSTM layer. This layer also accepts an $a \times b$ matrix, denoted by $\mathbf{X}'' = [\mathbf{f}_i]_{i=1}^a$, which is the output of the input layer. Each LSTM layer contains a memory cells, thus there are a total of $2a$ cells in the forward layer and the backward layer. Each row vector f_i of \mathbf{X}'' is input to one of the LSTM cells both in the forward layer and the backward layer.

$$G_i^f = \alpha(\mathbf{W}_i^f \mathbf{f}_i + \mathbf{U}_i^f \mathbf{h}_{i-1} + \mathbf{b}_i^f) \quad (17)$$

$$G_i^u = \alpha(\mathbf{W}_i^u \mathbf{f}_i + \mathbf{U}_i^u \mathbf{h}_{i-1} + \mathbf{b}_i^u) \quad (18)$$

$$G_i^o = \alpha(\mathbf{W}_i^o \mathbf{f}_i + \mathbf{U}_i^o \mathbf{h}_{i-1} + \mathbf{b}_i^o) \quad (19)$$

$$\tilde{\Theta}_i = \beta(\mathbf{W}_i^\theta \mathbf{f}_i + \mathbf{U}_i^\theta \mathbf{h}_{i-1} + \mathbf{b}_i^\theta) \quad (20)$$

$$\Theta_i = G_i^f \odot \Theta_{i-1} + G_i^u \odot \tilde{\Theta}_i \quad (21)$$

$$\mathbf{h}_i = G_i^o \odot \gamma(\Theta_i) \quad (22)$$

Formula 17-22 describe the computing process after a row vector f_i is fed to an LSTM cell, where $i \in \mathbb{N}^+$, $i \leq a$. Θ is the cell state vector and $\tilde{\Theta}$ is the cell input activation vector. The initial Θ_0 is a zero vector of size h (hidden units of each LSTM cell). G represents “gate” in a cell. G_i^f is the forget gate. G_i^u is the update gate, which is also called the input gate. G_i^o is the output gate. $\mathbf{W} \in \mathbb{R}^{h \times b}$, $\mathbf{U} \in \mathbb{R}^{h \times h}$ are weight matrices and $\mathbf{b} \in \mathbb{R}^h$ is a bias vector parameter. All of \mathbf{W} , \mathbf{U} and \mathbf{b} need to be learned during training. The elements in \mathbf{W} , \mathbf{U} and \mathbf{b} can be treated as any real number \mathbb{R} . The superscript represents their shape. The activation functions, α , β and γ , can be treated as tanh, sigmoid or others. The hidden state vector \mathbf{h} , is also known as the output vector of an LSTM cell, whose size is h and the initial \mathbf{h}_0 is a zero vector. The operator \odot denotes the Hadamard product (element-wise product) [49].

For a bidirectional LSTM, the forward layer finally outputs an \mathbf{h}_a^f , and the backward layer also outputs an \mathbf{h}_a^b . The final output of BiLSTM is the direct sum of the two outputs through $\mathbf{h}_a^f \oplus \mathbf{h}_a^b$ [50], denoted by \mathbf{h}' .

⁶<https://js.tensorflow.org/api/latest/#layers.masking>

The output of the BiLSTM layer is eventually passed to the output layer, which is a multi-label classification dense layer. It accepts a vector of $2h$ size, which is \mathbf{h}' .

$$\mathbf{y} = \text{sigmoid}(\mathbf{W}_c \mathbf{h}' + \mathbf{b}) \quad (23)$$

In Formula 23, we perform binary classification on each category (label) through a sigmoid function. \mathbf{W}_c is an $l \times 2h$ weight matrix, where $2h$ is the size of input vector \mathbf{h}' and l is the number of target labels. Therefore, the final output is a vector $\mathbf{y} = [y_1, y_2, \dots, y_l]$ and the value of each element in it indicates the probability of the existence of each intent category. For each element y_i in \mathbf{y} , we let $y_i \geq 0.5$ be equal to 1 while $y_i < 0.5$ be equal to 0. A multi-hot vector is then generated, where 1 indicates the existence of one intent and 0 indicates the absence of such intent. So far, the intent detection of a smart contract is completed.

VI. EVALUATION

In this section, evaluation metrics and baselines are firstly described. Then we state the details of our experiment, including the configurations and results. Finally, we propose three research questions (RQs) and answer them according to the results of our experiment.

A. Evaluation Metrics

To evaluate our model, we present the confusion matrix:

- **True Positive (TP)**: the number of correctly predicted intent categories existing in smart contracts.
- **True Negative (TN)**: the number of correctly predicted non-existing intent categories in smart contracts.
- **False Positive (FP)**: the number of incorrectly predicted intent categories existing in smart contracts.
- **False Negative (FN)**: the number of incorrectly predicted non-existing intent categories in smart contracts.

With **TP**, **TN**, **FP** and **FN**, we can compute the metrics like accuracy, precision, recall and f1-score (F1) as Formula 24-27.

$$\text{accuracy} = \frac{\text{TP} + \text{TN}}{\text{TP} + \text{FP} + \text{FN} + \text{TN}} \quad (24)$$

$$\text{precision} = \frac{\text{TP}}{\text{TP} + \text{FP}} \quad (25)$$

$$\text{recall} = \frac{\text{TP}}{\text{TP} + \text{FN}} \quad (26)$$

$$\text{F1} = \frac{2 \times \text{precision} \times \text{recall}}{\text{precision} + \text{recall}} \quad (27)$$

Accuracy is a basic metric for model evaluation, describing the proportion of correct predictions in total predictions. Precision is a measure of how many of the positive predictions made are correct. Recall is a measure of how many of the positive cases the classifier correctly predicted, over all the positive cases in the data. F1 is a measure combining both precision and recall.

TABLE II
BASELINES COMPARISON

Model	Accuracy	Precision	Recall	F1-score
SMARTINTENTNN				
Rank ASC	0.9437	0.8079	0.7960	0.8019
Scale×2	0.9474	0.8173	0.8142	0.8158
Scale×4	0.9455	0.8380	0.7677	0.8013
Scale×10	0.9435	0.8250	0.7682	0.7956
Scale×2 dropout	0.9482	0.8118	0.8308	0.8212
Other Models				
LSTM	0.9405	0.8126	0.7588	0.7848
BiLSTM	0.9402	0.8033	0.7706	0.7866
CNN	0.9309	0.8395	0.6392	0.7258

B. Baselines

As this is the first work on smart contract intent detection, we have no previous related work to compare. We perform a self-comparison with three baselines, respectively, using a basic LSTM model, a BiLSTM model, a CNN (Convolutional Neural Network) model [51] to detect the intents in smart contracts. There are two variants of the intent highlight model: rank and scale. Of the two variants, a scale can be further multiplied by different constants. We add a dropout layer [52] to the best variant (*i.e.*, $2 \times$ scale intent highlight). Therefore, we finally list eight different control groups in Table II.

C. Experiment Details

We first state the experimental configurations in our model training. All the models are built and trained on Tensorflow.js. We prepare the first 10,000 rows of data in our database to train the model and employ the data after 20,000 to evaluate the model. The middle 10,000 rows of data are standby, which can be used for extended training or evaluation. Each training batch size is 20 smart contracts, and they are shuffled during training. The number of training epochs is 30, which means that we train the neural network with all the training data for 30 cycles. We take “binaryCrossentropy” and “Adam” as the loss function and optimizer respectively. The number of hidden units in LSTM is set to 32 as 32 is the best parameter achieved by repeated tuning. We have also tried 16, 64, 128, 256 and 512 hidden units for an LSTM cell while their performance is not as good as 32. The dimension of output multi-hot vectors \mathbf{y} in Section V.C is 10 as we label ten categories of intents.

Fig. 7 lays out the trend charts of the metrics as each model is evaluated with 10,000 smart contracts. We find that after about 7,000 evaluations, the metrics tend to be steady. Therefore, we consider that the metrics evaluated on 10,000 smart contracts are reasonable and reliable. In Fig. 7, **AC**, **PR** and **RE** are abbreviations of accuracy, precision, and recall, respectively.

We also conduct a specific experiment on the intent highlight model. Referring to Fig. 8, we visualize the outputs of the intent highlight model. In Fig. 8, (a) shows an entire visualization of the intent highlight performed on a smart contract. After myriad experiments, we find that the most appropriate k

RQ3 How is the capability of SMARTINTENTNN in detecting different categories of intents?

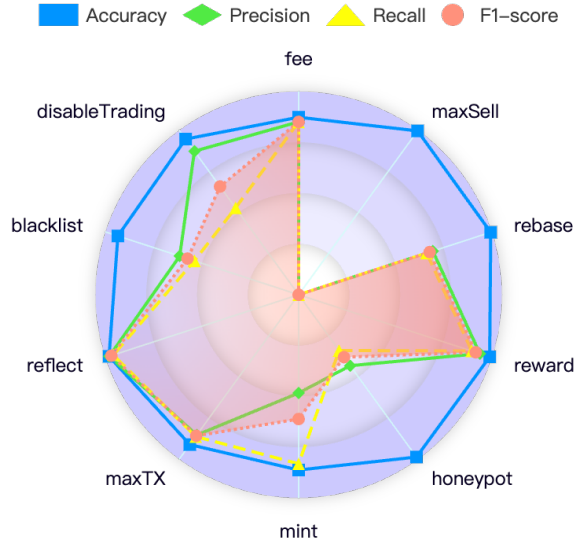


Fig. 9. Evaluation metrics of SMARTINTENTNN for different intents.

The performance of SMARTINTENTNN in detecting different types of intents is different. As shown in Fig. 9, we separately evaluate our model on each category of intent and reach the different metrics. Among all the intents, SMARTINTENTNN performs outstandingly in detecting **fee**, **reflect** and **maxTX** three intents while the F1 of **maxSell** detection is poor. According to the statistics in Section IV, it is not difficult to analyze that the reason for this gap is that, in our dataset, there are too few samples (only 0.05%) of **maxSell** while the proportion of **fee**, **reflect** and **maxTX** are very high (see the explanation of threats to validity in Section VI.E). Despite the relatively weak efficiency in detecting a few types of intents, the accuracy metric of each one is still high, over 90%, which demonstrates most of the risky intents detected by our model are correct.

E. Threats to Validity

There is a threat from the imbalance of dataset, *e.g.*, **maxSell**, according to the statistics in Section IV, only accounting for 0.05%, far less than the other labels of intents. The data scarcity issue can result in our model being unable to learn their representations well. We find these intents rare in nature as we collect smart contracts wildly and randomly on the real blockchain. Nevertheless, SMARTINTENTNN is a trainable model, as long as the case number of these intents increases in smart contracts, we can perform model retraining to improve the detection capability of these intents.

Another threat is the universality of our model, as all our data is from BSC. BSC is an Ethereum-like blockchain, as well as it supports EVM and Solidity. Therefore, the model trained on BSC can detect smart contracts not only on BSC but also on Ethereum and other Ethereum-like blockchains. Although our

model currently does not sustain detecting the smart contracts not in Solidity, we can still perform the additional training on other smart contract programming languages, *e.g.*, JavaScript, and Vyper [53], to drive our model to sustain them. As we know, Solidity is the most popular and universal programming language for smart contracts [54], thus we consider that our current model is already universal for detecting most of the smart contracts on various blockchains.

VII. RELATED WORK

In this section, we introduce the related work from the perspective of external risks and internal risks, as well as discuss the distinctions between their work and ours.

A. External Risks

A survey of smart contract vulnerabilities [20] well summarizes various vulnerabilities on Ethereum, as well as the applied attacks and defense methods. The earlier vulnerability detection research typically performs static [16], [17], [55]–[58] or dynamic analysis [59] on smart contracts. A kind of datalog-based formulation is used in [19] to perform the static analysis over EVM execution traces. TETHER [60] finds vulnerable execution traces in smart contracts, as well as employs symbolic execution to create exploits for them. Besides, Oyente [18], Securify [58] and Maian [61] also adopt symbolic executions to find vulnerability traces. SMARTSHIELD [62] detects security-related bugs by analyzing the abstract syntax tree (AST) and EVM bytecode. The latest research [63], [64] also applies deep learning to detect vulnerabilities in smart contracts. The above work aims to detect the external risks, mainly the exploitation of vulnerabilities, while our research aims to detect the internal risks from the developers’ intent.

B. Internal Risks

The first empirical analysis of Bitcoin-based scams is presented by [65]. HONEYBADGER [22] is built to expose honeypots through symbolic execution with the well-defined heuristics. “Trade or Trick” [24] proposes an approach for flagging scam tokens on Uniswap based on a guilt-by-association heuristic and a machine-learning-powered technique. Its ground truth is labeled by official tokens and scam tokens, which is different from our intent labels. SCSGuard [66] is the most relevant to our work, which uses deep learning to detect scams in smart contracts. The difference is that: (i) the target of its detection is Ponzi and honeypots; (ii) it learns from the bytecode rather than the smart contract source code. Despite being the same in detecting internal risks, our approach is the first work to implement the detection by identifying the developers’ intents in smart contracts.

VIII. CONCLUSION

We propose a new automated approach, to detect the developers’ intent in smart contracts. To implement the approach, we build an automated smart contract intent detection model, namely SMARTINTENTNN, consisting of a universal sentence encoder, an intent highlight model based on K-means, and a

DNN integrated with a BiLSTM layer. For training this model, we collect more than 40,000 smart contracts, clean the data, and label them with ten typical categories of intents. According to the experimental results, we find that the performance of our model performs better than all baselines, up to the accuracy of 0.9482, the precision of 0.8118, the recall of 0.8308, and the f1-score of 0.8212.

In the future, our work will focus on two aspects to improve this model: (i) train the model for smart contracts in other programming languages; (ii) build an programming language encoder specifically for generating smart contract embeddings.

IX. DATA AVAILABILITY

SMARTINTENTNN is available online. To use our source code and dataset, please refer to the documentation on the following website.

<https://gitlab.com/web3se/smartintent>

REFERENCES

- [1] "Introduction to web3." [Online]. Available: <https://ethereum.org/en/web3>
- [2] U. W. Chohan, "Web 3.0: The future architecture of the internet?" Available at SSRN, 2022.
- [3] S. Richards, "Web2 vs web3." [Online]. Available: <https://ethereum.org/en/developers/docs/web2-vs-web3>
- [4] V. Buterin *et al.*, "A next-generation smart contract and decentralized application platform," *white paper*, vol. 3, no. 37, pp. 2–1, 2014.
- [5] G. Wood *et al.*, "Ethereum: A secure decentralised generalised transaction ledger," *Ethereum project yellow paper*, vol. 151, no. 2014, pp. 1–32, 2014.
- [6] "Ethereum." [Online]. Available: <https://ethereum.org>
- [7] M. Nofer, P. Gomber, O. Hinz, and D. Schiereck, "Blockchain," *Business & Information Systems Engineering*, vol. 59, no. 3, pp. 183–187, 2017.
- [8] M. Röscheisen, M. Baldonado, K. Chang, L. Gravano, S. Ketchpel, and A. Paepcke, "The stanford infobus and its service layers: Augmenting the internet with higher-level information management protocols," *Digital Libraries in Computer Science: The MeDoc Approach*, pp. 213–230, 1998.
- [9] B. P. P. Martin Fries, *Smart Contracts*. Mohr Siebeck GmbH and Co. KG, 2019. [Online]. Available: <http://www.jstor.org/stable/j.ctvn96h9r>
- [10] A. Savelyev, "Contract law 2.0: 'smart' contracts as the beginning of the end of classic contract law," *Information & communications technology law*, vol. 26, no. 2, pp. 116–134, 2017.
- [11] D. Tapscott and A. Tapscott, *Blockchain revolution: how the technology behind bitcoin is changing money, business, and the world*. Penguin, 2016.
- [12] N. Szabo, "Smart contracts: building blocks for digital markets," *EXTROPY: The Journal of Transhumanist Thought*, (16), vol. 18, no. 2, p. 28, 1996.
- [13] "Introduction to smart contracts." [Online]. Available: <https://ethereum.org/en/developers/docs/smart-contracts>
- [14] I.-A. BUCULEI *et al.*, "Information systems vulnerabilities," in *International Conference on Cybersecurity and Cybercrime*, vol. 4, 2017, pp. 39–48.
- [15] D. Siegel, "Understanding the dao attack." [Online]. Available: <http://www.coindesk.com/understanding-dao-hack-journalists>
- [16] L. Brent, A. Jurisevic, M. Kong, E. Liu, F. Gauthier, V. Gramoli, R. Holz, and B. Scholz, "Vandal: A scalable security analysis framework for smart contracts," *arXiv preprint arXiv:1809.03981*, 2018.
- [17] S. Kalra, S. Goel, M. Dhawan, and S. Sharma, "Zeus: analyzing safety of smart contracts," in *Ndss*, 2018, pp. 1–12.
- [18] L. Luu, D.-H. Chu, H. Olickel, P. Saxena, and A. Hobor, "Making smart contracts smarter," in *Proceedings of the 2016 ACM SIGSAC conference on computer and communications security*, 2016, pp. 254–269.
- [19] D. Perez and B. Livshits, "Smart contract vulnerabilities: Does anyone care?" *arXiv preprint arXiv:1902.06710*, pp. 1–15, 2019.
- [20] D. He, Z. Deng, Y. Zhang, S. Chan, Y. Cheng, and N. Guizani, "Smart contract vulnerability analysis and security audit," *IEEE Network*, vol. 34, no. 5, pp. 276–282, 2020.
- [21] K. Li, J. Chen, X. Liu, Y. R. Tang, X. Wang, and X. Luo, "As strong as its weakest link: How to break blockchain dapps at rpc service." in *NDSS*, 2021.
- [22] C. F. Torres, M. Steichen *et al.*, "The art of the scam: Demystifying honeypots in ethereum smart contracts," in *28th USENIX Security Symposium (USENIX Security 19)*, 2019, pp. 1591–1607.
- [23] J. Wu, Q. Yuan, D. Lin, W. You, W. Chen, C. Chen, and Z. Zheng, "Who are the phishers? phishing scam detection on ethereum via network embedding," *IEEE Transactions on Systems, Man, and Cybernetics: Systems*, 2020.
- [24] P. Xia, H. Wang, B. Gao, W. Su, Z. Yu, X. Luo, C. Zhang, X. Xiao, and G. Xu, "Trade or trick? detecting and characterizing scam tokens on uniswap decentralized exchange," *Proceedings of the ACM on Measurement and Analysis of Computing Systems*, vol. 5, no. 3, pp. 1–26, 2021.
- [25] "What is a smart contract security audit? a beginner's guide." [Online]. Available: <https://cointelegraph.com/blockchain-for-beginners/what-is-a-smart-contract-security-audit-a-beginners-guide>
- [26] S. Hochreiter and J. Schmidhuber, "Long short-term memory," *Neural computation*, vol. 9, no. 8, pp. 1735–1780, 1997.
- [27] I. Sutskever, O. Vinyals, and Q. V. Le, "Sequence to sequence learning with neural networks," *Advances in neural information processing systems*, vol. 27, 2014.
- [28] M. Abadi, P. Barham, J. Chen, Z. Chen, A. Davis, J. Dean, M. Devin, S. Ghemawat, G. Irving, M. Isard *et al.*, "Tensorflow: a system for large-scale machine learning," in *12th USENIX symposium on operating systems design and implementation (OSDI 16)*, 2016, pp. 265–283.
- [29] D. Smilkov, N. Thorat, Y. Assogba, C. Nicholson, N. Kreeger, P. Yu, S. Cai, E. Nielsen, D. Soegel, S. Bileschi *et al.*, "Tensorflow.js: Machine learning for the web and beyond," *Proceedings of Machine Learning and Systems*, vol. 1, pp. 309–321, 2019.
- [30] "Solidity." [Online]. Available: <https://soliditylang.org/>
- [31] D. Cer, Y. Yang, S.-y. Kong, N. Hua, N. Limtiaco, R. S. John, N. Constant, M. Guajardo-Cespedes, S. Yuan, C. Tar *et al.*, "Universal sentence encoder," *arXiv preprint arXiv:1803.11175*, 2018.
- [32] Chainalysis, "The 2022 crypto crime report," Chainalysis Inc., Tech. Rep., 2022. [Online]. Available: <https://go.chainalysis.com/2022-Crypto-Crime-Report.html>
- [33] "Rug pull." [Online]. Available: <https://academy.binance.com/en/glossary/rug-pull>
- [34] "Ethereum virtual machine (evm)." [Online]. Available: <https://ethereum.org/en/developers/docs/evm>
- [35] Q. Wang, R. Li, Q. Wang, and S. Chen, "Non-fungible token (nft): Overview, evaluation, opportunities and challenges," *arXiv preprint arXiv:2105.07447*, 2021.
- [36] T. Mikolov, I. Sutskever, K. Chen, G. S. Corrado, and J. Dean, "Distributed representations of words and phrases and their compositionality," *Advances in neural information processing systems*, vol. 26, 2013.
- [37] K. W. Church, "Word2vec," *Natural Language Engineering*, vol. 23, no. 1, pp. 155–162, 2017.
- [38] J. Pennington, R. Socher, and C. D. Manning, "Glove: Global vectors for word representation," in *Proceedings of the 2014 conference on empirical methods in natural language processing (EMNLP)*, 2014, pp. 1532–1543.
- [39] H. Palangi, L. Deng, Y. Shen, J. Gao, X. He, J. Chen, X. Song, and R. Ward, "Deep sentence embedding using long short-term memory networks: Analysis and application to information retrieval," *IEEE/ACM Transactions on Audio, Speech, and Language Processing*, vol. 24, no. 4, pp. 694–707, 2016.
- [40] T. Mikolov, K. Chen, G. Corrado, and J. Dean, "Efficient estimation of word representations in vector space," *arXiv preprint arXiv:1301.3781*, 2013.
- [41] A. Vaswani, N. Shazeer, N. Parmar, J. Uszkoreit, L. Jones, A. N. Gomez, E. Kaiser, and I. Polosukhin, "Attention is all you need," *Advances in neural information processing systems*, vol. 30, 2017.
- [42] M. Iyyer, V. Manjunatha, J. Boyd-Graber, and H. Daumé III, "Deep unordered composition rivals syntactic methods for text classification," in *Proceedings of the 53rd annual meeting of the association for computational linguistics and the 7th international joint conference on*

- natural language processing (volume 1: Long papers)*, 2015, pp. 1681–1691.
- [43] F. A. Gers, J. Schmidhuber, and F. Cummins, “Learning to forget: Continual prediction with lstm,” *Neural computation*, vol. 12, no. 10, pp. 2451–2471, 2000.
- [44] S. Hochreiter and J. Schmidhuber, “Lstm can solve hard long time lag problems,” *Advances in neural information processing systems*, vol. 9, 1996.
- [45] Y. Bengio, A. Courville, and P. Vincent, “Representation learning: A review and new perspectives,” *IEEE transactions on pattern analysis and machine intelligence*, vol. 35, no. 8, pp. 1798–1828, 2013.
- [46] J. MacQueen, “Classification and analysis of multivariate observations,” in *5th Berkeley Symp. Math. Statist. Probability*, 1967, pp. 281–297.
- [47] K. Krishna and M. N. Murty, “Genetic k-means algorithm,” *IEEE Transactions on Systems, Man, and Cybernetics, Part B (Cybernetics)*, vol. 29, no. 3, pp. 433–439, 1999.
- [48] F. Rahutomo, T. Kitasuka, and M. Aritsugi, “Semantic cosine similarity,” in *The 7th international student conference on advanced science and technology ICAST*, vol. 4, no. 1, 2012, p. 1.
- [49] R. A. Horn and C. R. Johnson, *Matrix analysis*. Cambridge university press, 2012.
- [50] C. Faith and E. A. Walker, “Direct sum representations of injective modules,” *J. Algebra*, vol. 5, no. 2, pp. 203–221, 1967.
- [51] Y. LeCun, Y. Bengio *et al.*, “Convolutional networks for images, speech, and time series,” *The handbook of brain theory and neural networks*, vol. 3361, no. 10, p. 1995, 1995.
- [52] N. Srivastava, G. Hinton, A. Krizhevsky, I. Sutskever, and R. Salakhutdinov, “Dropout: a simple way to prevent neural networks from overfitting,” *The journal of machine learning research*, vol. 15, no. 1, pp. 1929–1958, 2014.
- [53] “Vyper.” [Online]. Available: <https://vyper.readthedocs.io>
- [54] “These are the top 10 programming languages in blockchain.” [Online]. Available: <https://thenextweb.com/news/javascript-programming-java-cryptocurrency>
- [55] T. Chen, X. Li, X. Luo, and X. Zhang, “Under-optimized smart contracts devour your money,” in *2017 IEEE 24th international conference on software analysis, evolution and reengineering (SANER)*. IEEE, 2017, pp. 442–446.
- [56] N. Grech, M. Kong, A. Jurisevic, L. Brent, B. Scholz, and Y. Smaragdakis, “Madmax: Surviving out-of-gas conditions in ethereum smart contracts,” *Proceedings of the ACM on Programming Languages*, vol. 2, no. OOPSLA, pp. 1–27, 2018.
- [57] S. Tikhomirov, E. Voskresenskaya, I. Ivanitskiy, R. Takhaviev, E. Marchenko, and Y. Alexandrov, “Smartcheck: Static analysis of ethereum smart contracts,” in *Proceedings of the 1st International Workshop on Emerging Trends in Software Engineering for Blockchain*, 2018, pp. 9–16.
- [58] P. Tsankov, A. Dan, D. Drachler-Cohen, A. Gervais, F. Buenzli, and M. Vechev, “Securify: Practical security analysis of smart contracts,” in *Proceedings of the 2018 ACM SIGSAC Conference on Computer and Communications Security*, 2018, pp. 67–82.
- [59] B. Jiang, Y. Liu, and W. K. Chan, “Contractfuzzer: Fuzzing smart contracts for vulnerability detection,” in *2018 33rd IEEE/ACM International Conference on Automated Software Engineering (ASE)*. IEEE, 2018, pp. 259–269.
- [60] J. Krupp and C. Rossow, “teether: Gnawing at ethereum to automatically exploit smart contracts,” in *27th USENIX Security Symposium (USENIX Security 18)*, 2018, pp. 1317–1333.
- [61] I. Nikolić, A. Kolluri, I. Sergey, P. Saxena, and A. Hobor, “Finding the greedy, prodigal, and suicidal contracts at scale,” in *Proceedings of the 34th annual computer security applications conference*, 2018, pp. 653–663.
- [62] Y. Zhang, S. Ma, J. Li, K. Li, S. Nepal, and D. Gu, “Smartshield: Automatic smart contract protection made easy,” in *2020 IEEE 27th International Conference on Software Analysis, Evolution and Reengineering (SANER)*. IEEE, 2020, pp. 23–34.
- [63] Y. Zhuang, Z. Liu, P. Qian, Q. Liu, X. Wang, and Q. He, “Smart contract vulnerability detection using graph neural network,” in *IJCAI*, 2020, pp. 3283–3290.
- [64] Z. Liu, P. Qian, X. Wang, Y. Zhuang, L. Qiu, and X. Wang, “Combining graph neural networks with expert knowledge for smart contract vulnerability detection,” *IEEE Transactions on Knowledge and Data Engineering*, 2021.
- [65] M. Vasek and T. Moore, “There’s no free lunch, even using bitcoin: Tracking the popularity and profits of virtual currency scams,” in *International conference on financial cryptography and data security*. Springer, 2015, pp. 44–61.
- [66] H. Hu, Q. Bai, and Y. Xu, “Scsguard: Deep scam detection for ethereum smart contracts,” in *IEEE INFOCOM 2022-IEEE Conference on Computer Communications Workshops (INFOCOM WKSHPS)*. IEEE, 2022, pp. 1–6.